Orthotropic hydraulic permeability of arrays of parallel cylinders

Mohsen Maleki,[1] Robert J. Martinuzzi,[2] Walter Herzog,[1] and Salvatore Federico[3,*]
[1]*Human Performance Laboratory and Department of Mechanical and Manufacturing Engineering, The University of Calgary, 2500 University Drive NW, Calgary, AB, Canada T2L 1N4*
[2]*Department of Mechanical and Manufacturing Engineering, The University of Calgary, 2500 University Drive NW, Calgary, AB, Canada T2L 1N4*
[3]*Department of Mechanical and Manufacturing Engineering and Human Performance Laboratory, The University of Calgary, 2500 University Drive NW, Calgary, AB, Canada T2L 1N4*
(Received 30 December 2016; revised manuscript received 6 July 2017; published 25 September 2017)

Approximate analytical methods are presented to calculate the overall orthotropic hydraulic permeability of a flow with low Reynolds number, passing through a bundle of parallel circular cylinders. Two particular distributions are considered: (i) arrays with ordered rectangular lattices and (ii) irregular nonrandom distributions for which the unit cell cross sections are elliptical. The standard unit cell models, originally developed by Happel and Kuwabara for a random distribution of cylinders, are adapted to the case of nonrandom distributions. The drag force on a representative cylinder in a direction perpendicular to its axis is obtained based on the standard unit cell model: the actual unit cell of rectangular or elliptical cross section is replaced with an "equivalent" cylindrical unit cell of diameter equal to the maximum width of the actual unit cell. Using the obtained drag forces and referring back to the original geometry of the unit cell, closed-form approximate expressions for the overall permeabilities in the perpendicular directions are obtained. Numerical comparisons with more sophisticated approaches confirm the good efficiency of the presented approach, especially in the range of low solid volume fraction, i.e., of high porosity. Previous studies have revealed that, for the parallel fluid flow, the variation of permeability with aspect ratio (or in general the lateral arrangement) of parallel cylinders is generally weak. These observations suggest that Happel's model for parallel permeability in a random distribution of cylinders could be a good approximation for parallel permeabilities in nonrandom distributions with the same volume fraction.

DOI: 10.1103/PhysRevE.96.033112

I. INTRODUCTION

Fluid flows across a bundle of parallel cylinders are commonly found in various examples, ranging from industrial applications (such as heat exchangers, filters, and fibrous porous materials) to biological applications (such as soft tissues, bones, and biomaterials). In view of this wide range of applications, several theoretical and experimental studies exist (see, e.g., Refs. [1–33]). Here, we confine our attention to creeping flow (i.e., flow with very low Reynolds number), which is particularly relevant to the permeability of fibrous biological tissues and biomaterials, with very low rate of fluid flow. The pioneering works of Happel [1] and Kuwabara [2] introduced classical methods for assessing the hydraulic permeability of parallel cylindrical arrays. An important idea in these works is adopting a unit cell model, in which the study of the flow through an array of cylinders is reduced to that of the flow in a unit cell. In both Happel's [1] and Kuwabara's [2] models, the unit cell consists of a representative cylinder surrounded by a cylindrical shell composed of fluid, with appropriate boundary conditions at the interface between the cylinder and surrounding fluid layer. The boundary conditions on the outer surface of the fluid layer in Happel's [1] and Kuwabara's [2] models are zero shear stress and zero vorticity, respectively. Both models are suitable for modeling random distributions of parallel cylinders, although Happel [1] seems to have had regular arrays in mind, as he was considering an application to heat exchangers.

Based on an "effective medium approximation" (EMA), Li and Park [34] calculated the normal and tangential permeabilities of parallel arrays of cylindrical fibers and also the overall permeability of a randomly orientated population of fibers. The key difference between the EMA model and the cell model of Happel [1] or Kuwabara [2] is that the fluid medium outside the cell boundary in the cell model is replaced by an effective porous medium whose permeability must be determined. Analogously to self-consistent homogenization methods, the compatibility of pressure gradients at the bulk and microscopic scales in the EMA results in a characteristic equation that can be solved for the overall permeability. However, in general, no closed-form permeability expression can be obtained from the EMA as the characteristic equation seems to be solvable only numerically. In addition, Li and Park [35] also considered the case in which the fibers are randomly distributed on planar planes. Numerical comparisons performed by Li and Park [35] indicate that the EMA, compared to the unit cell models of Happel [1] or Kuwabara [2], has the key benefit of predicting more accurate results at smaller porosities (i.e., larger solid volume fraction).

We note that Happel's [1], Kuwabara's [2], and Li and Park's [35] models are all based on a unit cell with circular cross section and a random distribution of parallel cylinders, and therefore do *not* capture any anisotropy in the plane perpendicular to the direction of the cylinders' axes, which would be imposed by any positional nonrandomness of cylinders.

Various applications in biological, chemical, and industrial examples require the study of fluid flow through parallel cylinders that have a nonrandom distribution, which adds to the complexity of the treatment. Particularly, much attention

*Corresponding author: salvatore.federico@ucalgary.ca

has been given to cylinders arranged on an ordered lattice, both theoretically and experimentally. In general, a fluid flow passing through an array of cylinders experiences an anisotropy in the overall permeability of the array. The two extreme possibilities are flow parallel and perpendicular to the axes of cylinders for which the overall permeabilities differ. In addition, the overall permeability of a fluid flow perpendicular to the axes may depend on the particular direction on the plane perpendicular to the axes. However, despite having a nonrandom distribution, due to their lattice symmetries, some arrays do not have any anisotropic overall permeability on the plane perpendicular to the cylinder axes. In other words, on average, the fluid flow permeability in any direction perpendicular to the axes is identical. For example, square, equilateral triangular, and hexagonal lattices show such a property. Thus, for these examples of ordered arrays, and of course for random arrays, the overall permeability tensor is transversely isotropic and has, in general, two distinct principal values, one associated with the cylindrical axis direction and the other associated with any direction perpendicular to the axis. An example of ordered lattice exhibiting nontransversely isotropic permeability is the rectangular lattice. For a rectangular lattice, the permeability tensor is in fact orthotropic, and possesses three principal values, two of them being perpendicular permeabilities associated with major and minor dimensions of the unit cell, and the third one being the parallel permeability associated with the direction of the cylinder axes.

Exact analytical study of fluid flow in arrays of cylinders in a regular lattice generally demands complicated mathematical manipulations. The analysis can become more complex, for example, when cylinders are assumed permeable. Thus, this problem has been numerically addressed extensively. Several lattices are studied as, in different applications, some lattices might be a preferred choice for designing (e.g., in heat exchangers) or for modeling porous materials (e.g., foams, filters, scaffolds, or biological tissues). Among the ordered lattices, much attention has been given to the square, equilateral triangular, and hexagonal ones, for which the overall permeability has no anisotropy on the plane perpendicular to the cylinder axes.

However, studies on permeability of rectangular lattices exist. Drummond and Tahir [6] studied fluid flow across arrays of cylinders on regular lattices (with boundary conditions of zero velocity on the surface and periodic boundary conditions, resulting in zero shear stress on the symmetry planes). Among their cases, they considered fluid flow parallel to the directions of cylinders for a rectangular array with aspect ratio (the ratio of the width and the length of the unit cell cross section) of two. Using eigenfunction expansion, collocation, and matching methods, Wang [20] analytically calculated the overall permeability of a system of parallel cylinders placed on a rectangular lattice for parallel and transverse (perpendicular) flow directions. Tamayol and Bahrami [26] used an analytical method to calculate the overall permeability of the fluid flow passing a bundle of parallel cylinders (fibers), arranged on regular lattices, parallel and perpendicular to the fiber axes. Their method relied on the assumption that the fluid velocity profile between the surfaces of adjacent cylinders is locally parabolic. Among the different lattices they studied, they considered a rectangular lattice for the fibers arrangement. DeValve and Pitchumani [36] implemented the method of boundary collocation to present a series solution for the parallel permeability of rectangular and staggered arrays of parallel cylinders.

In some physical systems, it appears that arrays of cylinders cannot be classified as either ordered (i.e., following a lattice) or random. To better understand such a case, assume that a group of parallel cylinders is randomly distributed. At the bulk scale, in contrast to an individual cylinder scale, the cylinders seem to be uniformly distributed. Now suppose that, for example, driven by an external source, cylinders are pushed or pulled in certain direction causing a directional bias in their placements. The directional bias at the bulk level causes an anisotropic state of permeability for a fluid flowing perpendicular to the axes of the cylinders. Conversely, for such an array, the directional bias can be canceled out by applying a hypothetical uniform deformation that transfers the array to a random one. In view of the kinematical considerations at the bulk level, an array that has such a property should have a unit cell with elliptical cross section. In the limiting case that an array is random, its unit cell has a circular cross section. Examples of unit cells with elliptical cross sections arise in deformed fibrous materials or materials with distributed cylindrical elements [37,38].

Quinn [37] and Quinn *et al.* [38] performed detailed analyses on the permeability of the proteoglycan matrix, which is a key component of articular cartilage. Their analyses involve considering a circular unit cell containing a cylindrical core (a glycosaminoglycan molecule) covered by a fluid layer. Assuming that the bulk deformation of tissue is directly transferred down to the micro level, they formulated the shape change of an originally circular unit cell to a unit cell with an elliptical cross section containing the same (rigid) circular cylindrical core. Adopting the elliptical unit cell and using perturbed versions of the unit cell models, they developed analytical solutions for the effective permeability tensor for the case that the shape of the unit cell cross section has a very small ellipticity. In fact, deriving an analytical solution for the overall permeability when the cross section of the unit cell has a finite ellipticity seems very challenging.

In many applications, especially where multiscale fluid flow analysis is involved, having closed-form permeability relations at different scales is extremely useful. When such expressions are available, the overall permeability of a multiscale material and the role of important variables at different scales can be conveniently studied. This work is motivated by our interest in modeling the proteoglycan matrix in articular cartilage, which is believed to play a major role in determining the permeability of the tissue (e.g., see Refs. [39,40]) and has a hierarchical structure, starting from proteoglycan aggregates, down to individual glycosaminoglycan molecules. This type of hierarchical structure is a suitable example of the applicability of analytical permeability relations at different scales.

The aim of the present work is to provide approximate analytical relations for the permeability of creeping fluid flow in nonrandom distributions of parallel cylinders for which permeability is orthotropic. Specifically, two cases will be studied:

(i) a rectangular array of parallel cylinders;

(ii) an array of cylinders having no ordered lattice, for which the cross section of the unit cell is elliptical; we refer to this array as an "irregular" (but not random) array.

By replacing the actual unit cell with equivalent circular unit cells of proper size, and implementing the standard unit cell models of Happel [1] or Kuwabara [2], the drag force applied on a representative cylinder in the perpendicular flow is obtained. Next, referring to the original cross-sectional area of the unit cell and following Happel [1] and Quinn [37], the overall permeabilities in two principal directions perpendicular to the direction of the axes of the cylinders are derived. The existing results and comparisons [6,7,26,36–38] show that the parallel permeability (compared to the perpendicular permeability) of a bundle of parallel cylinders has a weak dependance on the particular arrangement of the cylinders or the shape of the unit cell, but a strong dependance on the solid volume fraction. Thus, Happel's [1] prediction for the parallel permeability of random distributions of parallel cylinders (circular unit cell model) can also be considered as a good approximation for noncircular unit cells especially for low solid volume fractions [7].

The technique presented here can be generalized to more complex cases, where, for example, the cylinders are permeable. While obtaining exact analytical overall permeability relations could be challenging, the proposed technique can be used to adapt existing solutions for random arrays to arrays with noncircular unit cell cross sections. This work provides an efficient method in studying the permeability of nonrandom arrays of cylinders, with the added benefit of being suitable for multiscale structures and materials.

The work is organized as follows. In Sec. II, we discuss rectangular and irregular arrays of cylinders and their corresponding rectangular and elliptical unit cells. Section III introduces the models of Happel [1] and Kuwabara [2] for the perpendicular flow and their relations for the perpendicular drag forces, from which we have obtained the perpendicular permeability relations for rectangular and elliptical unit cells. Section IV presents the results available in the literature for parallel permeability. The results of our model are presented in Sec. V, along with comparisons with models available in the literature. A summary is provided in Sec. VI.

II. DISTRIBUTIONS OF CYLINDERS AND CORRESPONDING UNIT CELLS

Consider an array of parallel, identical, infinitely long circular cylinders of radius a, and let the free space among the cylinders be filled with an incompressible, Newtonian, viscous fluid with dynamic viscosity μ. Consider two cases of distribution of cylinders.

In the first case, the cylinders are arranged on a regular rectangular lattice [Fig. 1(a)]. The lattice is defined by the length d and the width ζd of a representative rectangular cell in the x and y directions, respectively. Obviously, ζ serves as the aspect ratio of the cell. Referring to the geometrical symmetries of the rectangular lattice, a unit cell of length d and width ζd can be realized with a representative cylinder placed at its center [Fig. 2(a)].

The second case considers an irregular array in which the cylinders have a positional bias in a certain direction. In general, this case can be obtained by "deforming" a region with a random distribution of parallel cylinders by means of a deformation with a nonzero *distortional* part (see the classical work by Flory [41]). A simple example is a uniaxial stretch in one direction. We start from a perfectly random distribution of cylinders over a referential square-shaped region of side L, as depicted in Fig. 1(b). Let us imagine to replace the cylinders by simply the points with coordinates (x_i, y_i) corresponding to the axes of the cylinders. Then, let us apply a uniform stretch λ in the direction y. As a result of this stretch, the new coordinates of the points will be $(x_i, \lambda y_i)$ and the region has become a rectangle with side L in the x direction and λL in the y direction. Finally, we place the cylinders in the deformed rectangular region, with the axes at the displaced positions $(x_i, \lambda y_i)$. The result is the region in Fig. 1(c): we can observe that, because of the bias in direction y caused by the stretch λ imposed on the referential square region, the cylinders are no longer randomly distributed and in fact are less dense in the y direction compared to the x direction.

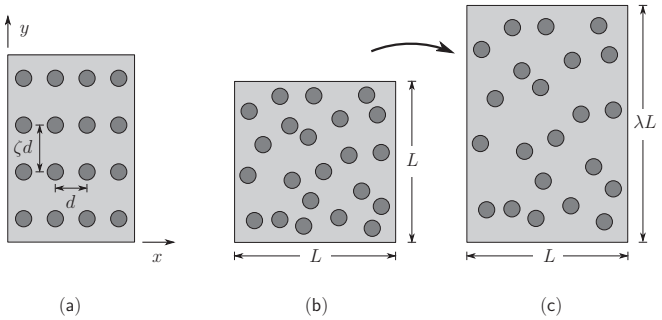

FIG. 1. (a) A rectangular array of parallel cylinders; (b) a hypothetical randomly distributed array of cylinders in a square region; (c) following a "deformation" in the y direction, the square region becomes rectangular and acquired a directional bias in the arrangement of cylinders.

For the random distribution of cylinders in the hypothetical "undeformed" square region [Fig. 1(b)], a natural choice for the unit cell in that configuration is a circular cylindrical, where a cylindrical core of radius a is located at its center, as considered, e.g., by Happel [1] and Kuwabara [2]. The outer radius b of the unit cell is chosen in such a way that the volume fraction of the solid phase within the unit cell matches the solid phase volume fraction f_0 of the bulk hypothetical region. Thus, the condition $f_0 = (a/b)^2$ is satisfied. The unit cell of the "undeformed" square region is shown in Fig. 2(b). The unit cell of the "deformed" rectangular region [Fig. 1(c)] is obtained

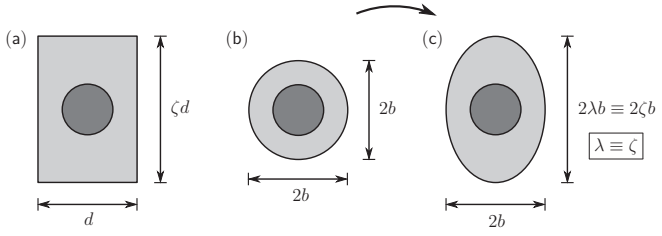

FIG. 2. (a) The rectangular unit cell of a rectangular array of parallel cylinders; (b) the circular unit cell of an irregular random distribution of cylinders; (c) the elliptical unit cell of an irregular non-random distribution of cylinders: the outer ellipse can be viewed as having been "deformed" from the outer circle of the circular unit cell depicted in panel (b).

from that of the "undeformed" square region [Fig. 1(b)] with a "deformation" process analogous to the one that brought the "undeformed" to the "deformed" region [Figs. 1(b) and 1(c)]. Thus, the outer circle of diameter b is deformed into an ellipse with semiaxes b in the x direction and λb in the y direction [Fig. 1(c)]. This implies that the outer boundary of the unit cell must be elliptical [37,38], and the aspect ratio ζ of the deformed unit cell coincides with the stretching parameter λ [37,38]. Under such condition, the solid volume fraction f in the deformed configuration can also be given as $f = f_0/\zeta$. It should be mentioned that, unlike the ordered rectangular arrays for which the unit cell [Fig. 2(a)] is an actual periodic part of the system, the unit cells for irregular arrays [Figs. 2(b) and 2(c)] do not represent any actual repeating subdomain of the system. This is naturally due to a lack of periodicity for irregular arrays. Thus, the approximation in dealing with irregular arrays starts at the stage of defining a "unit cell."

III. PERPENDICULAR PERMEABILITY RELATIONS

At the bulk level, the system of cylinders behaves like a saturated porous medium with an anisotropic permeability tensor $\boldsymbol{\kappa}$. As depicted in Fig. 1, assume that for the rectangular distribution the axes x and y are oriented in the lattice directions and, for the irregular distribution, the axes x and y are perpendicular to the cylindrical axes while the axis y is oriented in the direction of the directional bias (which was obtained by the fictitious stretch described in Sec. II). Thus, at the bulk level, the three xy, xz, and yz planes are the three planes of material symmetry for both rectangular and irregular distributions. This implies that the permeability tensor $\boldsymbol{\kappa}$ is, in general, orthotropic, having three distinct principal values. Also at the level of the unit cell, the geometrical symmetries (Fig. 2) imply that the three axes x, y, and z are the three principal axes of the overall permeability tensors $\boldsymbol{\kappa}$. The principal permeability values associated with these principal axes are denoted by κ_x, κ_y, and κ_z, respectively.

To derive the perpendicular permeability relations, we propose to replace a noncircular cell with an *equivalent* circular one, for which analytical solutions exist (e.g., those by Happel [1] and Kuwabara [2]). This approach allows for finding an approximated solution to the problem, which is simpler than attempting to find an analytical solution for noncircular unit cells *directly*. In the models by Happel [1] and Kuwabara [2], a creeping flow passing a system of parallel cylinders with random distribution is replaced by a flow passing a unit cell of circular cross section. For the flow perpendicular to the axes of cylinders, Happel [1] and Kuwabara [2] derived the drag forces applied to a representative cylinder. The two models differ for the boundary conditions at the outer surface of the unit cell: while Happel's model requires vanishing of the shear stress, Kuwabara's model requires satisfaction of zero vorticity. Happel [1] and Kuwabara [2] provided the following expressions for the perpendicular drag force $F_\perp$ on the cylinder,

$$F_\perp = 4\pi\mu U\left[\ln(b/a) - \frac{1}{2}\left(\frac{b^4-a^4}{b^4+a^4}\right)\right]^{-1} \quad \text{(Happel [1])} \tag{1}$$

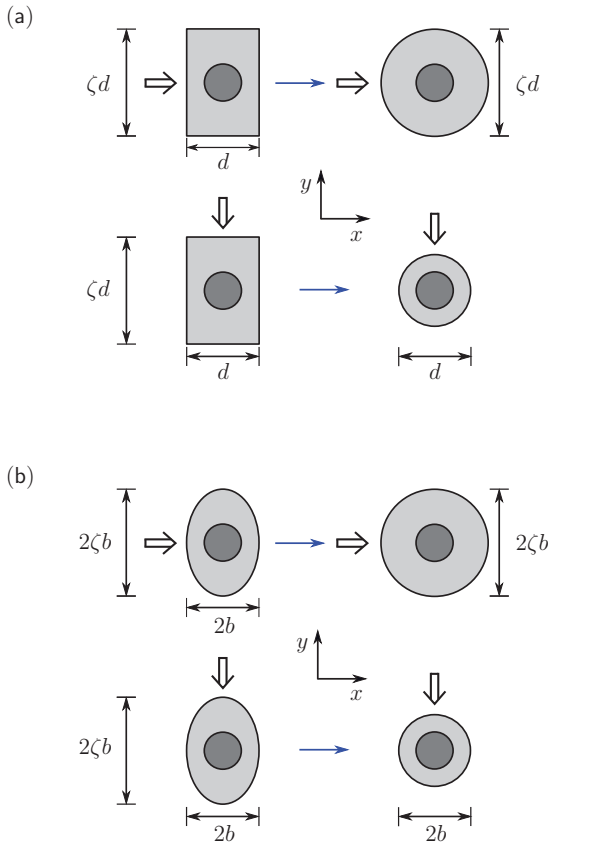

FIG. 3. Unit cells with rectangular [left column in panel (a)] and elliptical [left column in panel (b)] cross sections and the equivalent unit cells with circular cross sections [right column in panels (a) and (b)] for two cases of perpendicular fluid flow: in x direction [the top rows in panels (a) and (b)], and in y direction [the bottom rows in panels (a) and (b)].

and

$$F_\perp = 4\pi\mu U\left[\ln(b/a) - \tfrac{3}{4} + (a/b)^2 - \tfrac{1}{4}(a/b)^4\right]^{-1} \quad \text{(Kuwabara [2])}, \tag{2}$$

where b and U denote the radius of the unit cell and the magnitude of the average fluid velocity in the porous medium, respectively. We remark that, in principle, any model for the drag force $F_\perp$ developed for a circular unit cell would be suitable for the equivalent unit cell (which is described in Fig. 3). Here, the classical models of Happel [1] and Kuwabara [2] are chosen due to their wide acceptance.

The drag force $F_\perp$ can be used to derive the effective permeability $\kappa_\perp$ in the perpendicular direction as [1]

$$\kappa_\perp = \frac{A_{\text{uc}}\mu U}{F_\perp}, \tag{3}$$

where $A_{\text{uc}} = \pi b^2$ is the cross-sectional area of the unit cell. Thus,

$$\kappa_\perp = \frac{b^2}{4}\left[\ln(b/a) - \frac{1}{2}\left(\frac{b^4-a^4}{b^4+a^4}\right)\right] \quad \text{(Happel [1])} \tag{4}$$

and

$$\kappa_\perp = \frac{b^2}{4}\left[\ln(b/a) - \frac{3}{4} + (a/b)^2 - \frac{1}{4}(a/b)^4\right] \quad \text{(Kuwabara [2])} \tag{5}$$

are the perpendicular permeability values of Happel [1] and Kuwabara [2], respectively. The analysis of Quinn [37] showed that Eq. (3) also holds for noncircular (such as rectangular and elliptical) unit cells. For such a case, $A_{\rm uc}$ and $F_\perp$ in Eq. (3) will be the cross-sectional area of the noncircular unit cell and the drag force on the core cylinder inside the noncircular unit cell, respectively [37].

The proposed method uses the closed-form expressions of unit cell models of Happel [1] and Kuwabara [2] for the drag force applied on a cylinder in arrays of parallel cylinders with noncircular unit cells. To illustrate how this is achieved, consider the scheme depicted in Fig. 3, where unit cells of rectangular shape or elliptical shape of aspect ratio ζ are studied. First, consider a uniform creeping flow of a viscous fluid of viscosity μ passing through a unit cell in the x direction with the average velocity U. To obtain the drag force on the core cylinder, the idea is to replace the unit cell of rectangular and elliptical cross sections with *equivalent* unit cells of circular cross sections with diameters ζd and $2\zeta b$, respectively. Thus, the equivalent unit cell effectively offers the same maximum channel width for the fluid flow in the x direction as the original unit cell of rectangular or elliptical cross section does [see the top rows in Figs. 3(a) and 3(b)]. Hence, the drag force F_x is obtained as

$$F_x = F_\perp|_{b=\zeta d/2} \tag{6}$$

for the rectangular distribution and

$$F_x = F_\perp|_{b=\zeta b} \tag{7}$$

for the irregular distribution. The perpendicular drag forces $F_\perp$ in Eqs. (6) and (7) are substituted from Eqs. (1) and (2) based on Happel's [1] and Kuwabara's [2] models, respectively.

An analogous strategy is used to study the fluid flow in the second principal direction y. For that case, the equivalent unit cells will have radii d and $2b$ for the original rectangular and elliptical unit cells, respectively [see the bottom rows in Figs. 3(a) and 3(b)]. Hence, the drag force F_y is obtained as

$$F_y = F_\perp, \tag{8}$$

with the perpendicular drag force $F_\perp$ given in Eqs. (1) and (2) based on Happel's [1] and Kuwabara's [2] models, respectively. When the drag forces F_x and F_y in the x and y directions are obtained, following Happel [1] and Quinn [37], they will be substituted in Eq. (3), leading to the overall permeabilities κ_x and κ_y in the x and y directions as

$$\kappa_x = \frac{A_{\rm uc}\mu U}{F_x}, \tag{9a}$$

$$\kappa_y = \frac{A_{\rm uc}\mu U}{F_y}, \tag{9b}$$

where, for the unit cells of rectangular and elliptical cross sections, the areal cross sections are $A_{\rm uc} = \zeta d^2$ and $A_{\rm uc} = \pi\zeta b^2$, respectively.

From now on, we will use the following terminology for the developed models:

(1) RHUC, for rectangular distributions based on Happel's [1] unit cell model;

(2) EHUC, for irregular distributions with elliptical unit cell cross sections based on Happel's [1] unit cell model;

(3) RKUC, for rectangular distributions based on Kuwabara's [2] unit cell model;

(4) EKUC, for irregular distributions with elliptical unit cell cross sections based on Kuwabara's [2] unit cell model.

A. Permeability relations for rectangular distribution

Following the aforementioned procedure, upon the use of Eqs. (6), (8), (9a), and (9b), the nondimensional permeability relations, developed based on Happel's [1] or Kuwabara's [2] unit cell models, for a rectangular lattice with solid volume fraction f and the aspect ratio ζ are derived as

$$\frac{\kappa_x}{4a^2} = \frac{-1}{32f}\left[\ln\left(\frac{4}{\pi\zeta}f\right) + \frac{1-\left(\frac{4}{\pi\zeta}f\right)^2}{1+\left(\frac{4}{\pi\zeta}f\right)^2}\right], \tag{10a}$$

$$\frac{\kappa_y}{4a^2} = \frac{-1}{32f}\left[\ln\left(\frac{4\zeta}{\pi}f\right) + \frac{1-\left(\frac{4\zeta}{\pi}f\right)^2}{1+\left(\frac{4\zeta}{\pi}f\right)^2}\right], \tag{10b}$$

for the RHUC model, and

$$\frac{\kappa_x}{4a^2} = \frac{-1}{32f}\left[\ln\left(\frac{4}{\pi\zeta}f\right) + \frac{3}{2} - \frac{8}{\pi\zeta}f + \frac{8}{\pi^2\zeta^2}f^2\right], \tag{11a}$$

$$\frac{\kappa_y}{4a^2} = \frac{-1}{32f}\left[\ln\left(\frac{4\zeta}{\pi}f\right) + \frac{3}{2} - \frac{8\zeta}{\pi}f + \frac{8\zeta^2}{\pi^2}f^2\right], \tag{11b}$$

for the RKUC model. It is noteworthy that κ_x and κ_y, for both RHUC and RKUC models, are interchanged when ζ and ζ^{-1} are interchanged (depicted in Fig. 5). This can be justified by the geometrical symmetries of the problem.

B. Permeability relations for irregular distribution

Upon use of Eqs. (7), (8), (9a), and (9b), the nondimensional permeability relations for an array of cylinders, with nonrandom and irregular distribution and a unit cell of elliptical cross section with aspect ratio ζ, can be derived using Happel's [1] or Kuwabara's [2] unit cell models as

$$\frac{\kappa_x}{4a^2} = \frac{-1}{32f}\left[\ln(\zeta^{-1}f) + \frac{1-(\zeta^{-1}f)^2}{1+(\zeta^{-1}f)^2}\right], \tag{12a}$$

$$\frac{\kappa_y}{4a^2} = \frac{-1}{32f}\left[\ln(\zeta f) + \frac{1-(\zeta f)^2}{1+(\zeta f)^2}\right], \tag{12b}$$

for the EHUC model, and

$$\frac{\kappa_x}{4a^2} = \frac{-1}{32f}\left[\ln(\zeta^{-1}f) + \frac{3}{2} - 2\zeta^{-1}f + \frac{1}{2}\zeta^{-2}f^2\right], \tag{13a}$$

$$\frac{\kappa_y}{4a^2} = \frac{-1}{32f}\left[\ln(\zeta f) + \frac{3}{2} - 2\zeta f + \frac{1}{2}\zeta^2 f^2\right], \tag{13b}$$

for the EKUC model. Similar to the case of the rectangular lattice, in the irregular lattice, κ_x and κ_y for both EHUC

and EKUC models are interchanged when ζ and ζ^{-1} are interchanged (depicted in Fig. 5).

IV. PARALLEL PERMEABILITY

Also, Happel [1], based on the same unit cell model, derived the following expression for the effective permeability $\kappa_\parallel$ for the fluid flow parallel to the axes of cylinders [1]:

$$\kappa_\parallel = \frac{1}{8b^2}[4a^2b^2 - a^4 - 3b^4 + 4b^4 \ln(b/a)]. \qquad (14)$$

Relation Eq. (14) can alternatively be expressed nondimensionally and in terms of the solid volume fraction $f = (a/b)^2$ as [1]

$$\frac{\kappa_\parallel}{4a^2} = \frac{1}{32f}(4f - f^2 - 3 - 2\ln f). \qquad (15)$$

Fluid flow parallel to arrays of parallel cylinder has been studied previously. However, compared to perpendicular permeabilities, the existing studies show insignificant variations of parallel permeabilities with the aspect ratio (or the lateral arrangement of fibers). Drummond and Tahir [6] showed the weak dependence of the parallel permeability $\kappa_\parallel$ to the particular arrangement of parallel cylinders and emphasized the primary role of the volume fraction. They also identified a similar structure for the parallel permeability relations among several types of unit cells. Jackson and James [7] compared the results of Drummond and Tahir [6] and Happel [1] and pointed out that different models show close agreement when their volume fractions are equal, and that Happel's [1] model can be a good approximation especially for small volume fractions. Also, Tamayol and Bahrami [26] observed a small dependence of the parallel permeability $\kappa_\parallel$ on the aspect ratio of rectangular arrays.

Figure 4 shows the results of Happel's model [1] compared to the results of rectangular arrays presented by Drummond and Tahir [6] (in which the aspect ratio is $\zeta = 2$), Wang [20] (in which several aspect ratios ζ are considered), and DeValve and Pitchumani [36] (for aspect ratios $\zeta = 1$, $\zeta = \tan 60^\circ$, and $\zeta = \tan 70^\circ$). It can be noted that the range of variations of the nondimensional parallel permeability $\kappa_z/(4a^2)$ among the different aspect ratios and models are not significant, in the sense that their values are in the same order of magnitude. The difference is particularly small for smaller volume fractions f. Also, the difference between Happel's model [1] and the other models becomes more evident for larger aspect ratios ζ.

It is also noteworthy that Quinn [37] and Quinn *et al.* [38], when studying the permeability of elliptical unit cells with infinitesimal ellipticity, observed that the deviatoric strain has no first-order contribution to the parallel permeability, implying that, when the area of the elliptical unit cell is fixed (which is equivalent to constancy of the volume fraction f), the parallel permeability κ_z of the unit cell is not sensitive to first-order geometrical changes.

In summary, following Drummond and Tahir [6] and Jackson and James [7], Happel's model [1] can represent a fair approximation for the parallel permeability for nonrandom distributions. This approximation has better predictions for smaller values of volume fractions f and aspect ratios ζ closer to unity.

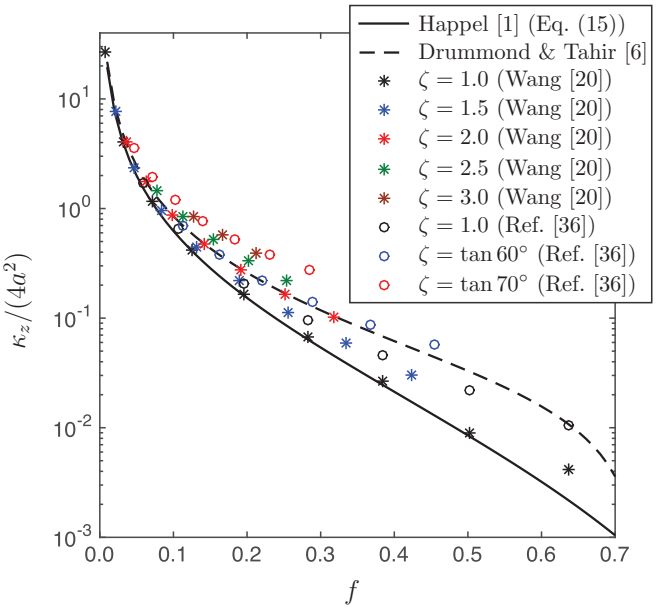

FIG. 4. Comparison of the variation of the nondimensional parallel permeability $\kappa_z/(4a^2)$ of Happel [1] (i.e., Eq. (15) of the present paper), and the results for rectangular arrays presented by Drummond and Tahir [6] (for aspect ratio $\zeta = 2$), Wang [20] (for aspect ratios $\zeta = 1$, $\zeta = 1.5$, $\zeta = 2$, $\zeta = 2.5$, and $\zeta = 3$), and the rectangular arrays presented by DeValve and Pitchumani [36] (for aspect ratios $\zeta = 1$, $\zeta = \tan 60^\circ$, and $\zeta = \tan 70^\circ$) versus the volume fraction f.

V. RESULTS AND DISCUSSIONS

In this section, numerical values of the perpendicular permeability are generated via the proposed permeability models and compared to those obtained via other models available in the literature. Depicted in Fig. 5 are the variations of the nondimensional perpendicular permeability components $\kappa_x/(4a^2)$ and $\kappa_y/(4a^2)$ versus the aspect ratio ζ. Comparisons are made between different unit cell models of rectangular and elliptical cross sections, i.e., the RHUC, RKUC, EHUC, and EKUC models, and selected values of volume fractions f. It is observed that, for $\zeta > 1$, we have $\kappa_x > \kappa_y$ while, for $\zeta < 1$, we have $\kappa_x < \kappa_y$, which is physically reasonable because, for a fixed volume fraction f, the permeability of a flow in a direction with a wider channel is larger. Thus, when the aspect ratio ζ increases, the x direction (y direction) permeability κ_x (κ_y) increases (decreases). In the limit $\zeta \to 1$ (i.e., a square or random array), κ_x and κ_y coincide.

It can be shown that, at a given volume fraction f, the aspect ratios of rectangular and elliptical unit cells must be limited as $4f/\pi \leqslant \zeta \leqslant \pi/(4f)$ for the rectangular unit cell [26], and $f \leqslant \zeta \leqslant 1/f$ for the elliptical unit cell. Beyond these limits, the neighboring cylinders intersect, which is not physically admissible. Figure 5 also reveals that, among the four models, the EHUC and RKUC models provide the largest and smallest permeability values, respectively (in both x and y directions). In addition, the RHUC and EHUC models always

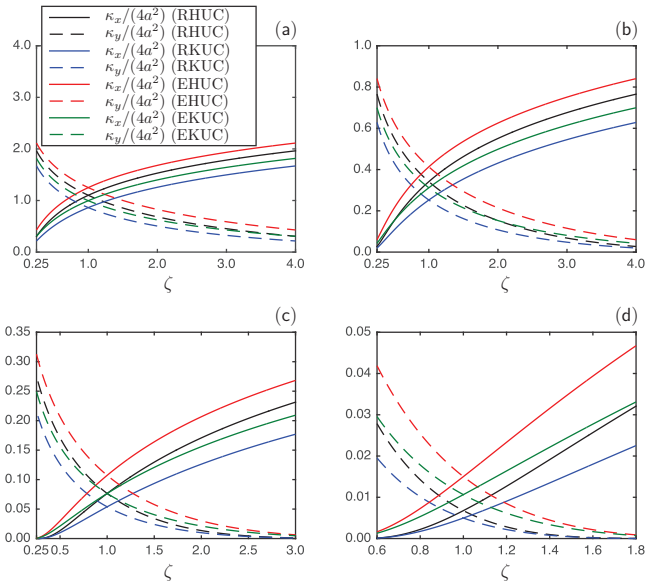

FIG. 5. Variations of the non-dimensional perpendicular permeability components $\kappa_x/(4a^2)$ and $\kappa_y/(4a^2)$ versus the aspect ratio ζ, based on the RHUC, RKUC, EHUC, and EKUC models, for selected values of volume fraction: (a) $f = 0.05$, (b) $f = 0.1$, (c) $f = 0.2$, and (d) $f = 0.4$.

predict larger permeability values, respectively, compared to the RKUC and EKUC models in both x and y directions.

Figure 6 shows the variations of the nondimensional perpendicular permeabilities $\kappa_x/(4a^2)$ and $\kappa_y/(4a^2)$ with the volume fraction f, for RHUC, RKUC, EHUC, and EKUC models, for selected aspect ratios ζ. It is observed that, when the volume fraction f increases, all permeability values (in both x and y directions) decrease. A change in the aspect ratio ζ does alter the values of the permeabilities, but otherwise it has no significant impact on their trends. Moreover, the observation made in Fig. 5 on the order of permeability values among different unit cell models and unit cell shapes also holds for the case of Fig. 6.

Comparisons of the variations of nondimensional permeabilities in directions x and y versus the volume fraction f

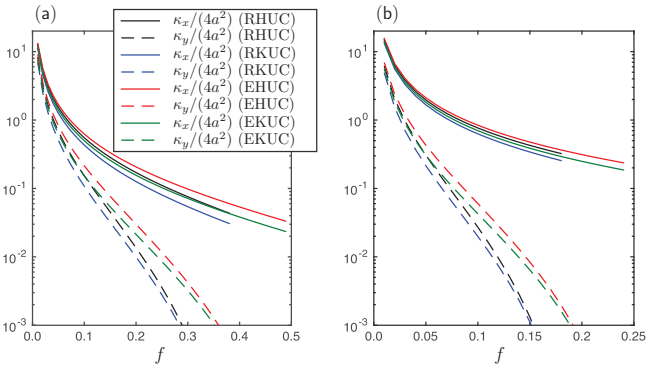

FIG. 6. Variations of the nondimensional perpendicular permeability components $\kappa_x/(4a^2)$ and $\kappa_y/(4a^2)$ versus the volume fraction f, based on the RHUC, RKUC, EHUC, and EKUC models, for selected values of the aspect ratio: (a) $\zeta = 2$ and (b) $\zeta = 4$.

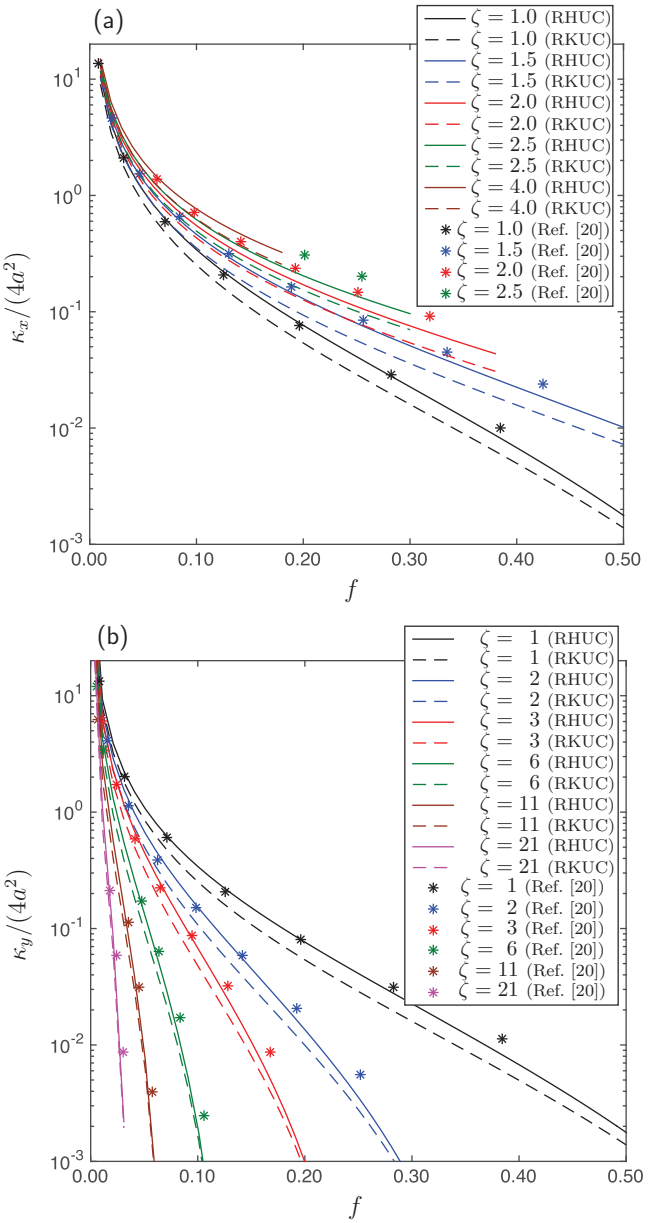

FIG. 7. (a) Variations of nondimensional perpendicular permeability component $\kappa_x/(4a^2)$ of RHUC and RKUC models [Eqs. (10a) and (11a)] versus volume fraction f for rectangular arrays and selected values of the aspect ratio, $\zeta = 1$, $\zeta = 1.5$, $\zeta = 2$, $\zeta = 2.5$, and $\zeta = 4$, and comparison with the results of Wang [20]. (b) Variations of the nondimensional perpendicular permeability component $\kappa_y/(4a^2)$ in the RHUC and RKUC models [Eqs. (10b) and (11b)] versus volume fraction f for rectangular arrays and selected values of the aspect ratio, $\zeta = 1$, $\zeta = 2$, $\zeta = 3$, $\zeta = 6$, $\zeta = 11$, and $\zeta = 21$, and comparison with the results of Wang [20].

for rectangular arrays, between relation Eqs. (10) and (11) and the results of Wang [20], are provided in Figs. 7(a) and 7(b), respectively. It can be observed that the permeability relation Eqs. (10) and (11) show good agreement with the analytical results of Wang [20], particularly for smaller values of the aspect ratio ζ and volume fraction f. In fact, most permeability values predicted by Eqs. (10) and (11) are slightly smaller than

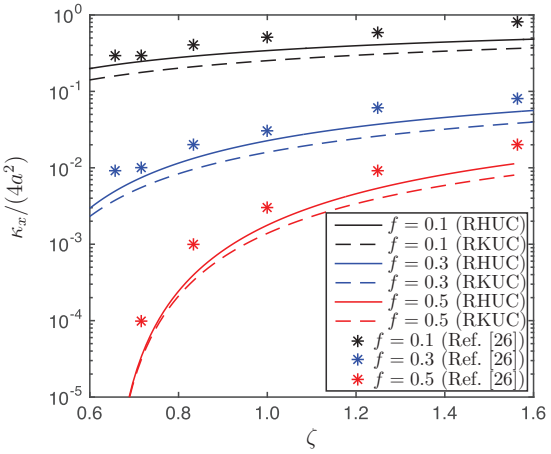

FIG. 8. Variation of the nondimensional perpendicular permeability component $\kappa_x/(4a^2)$ in the RHUC and RKUC models [Eqs. (10a) and (11a)] versus the aspect ratio ζ, for selected values of volume fraction, $f = 0.1$, $f = 0.3$, and $f = 0.5$, and comparison with the results of Tamayol and Bahrami [26].

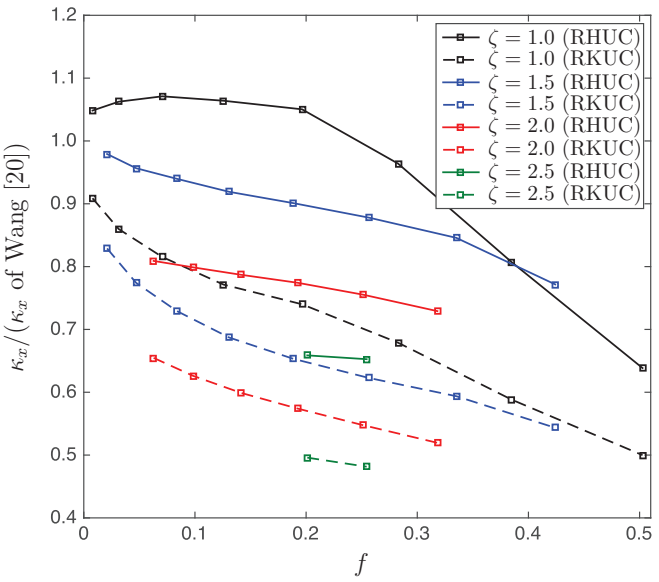

FIG. 9. Variation of the ratio $\kappa_x/(\kappa_x$ of Wang [20]) of the perpendicular permeability component κ_x, in the RHUC and RKUC, and the perpendicular permeability component κ_x of Wang [20], with volume fraction f for selected values of the aspect ratio ζ.

the corresponding values predicted by Wang [20]. However, the trends of the results between the presented methods and Wang's [20] are very close.

Figure 8 presents a comparison between $\kappa_x/(4a^2)$, given in Eqs. (10a) (RHUC model) and (11a) (RKUC model) for rectangular arrays, and the results of Tamayol and Bahrami [26], as functions of the aspect ratio ζ, for selected values of the volume fraction f. Fairly good agreement exists between the predicted results and those of Tamayol and Bahrami [26]; the agreement is slightly better for smaller volume fractions f. Also, relation Eqs. (10a) and (11a) predict smaller permeability values compared to the those by Tamayol and Bahrami [26]. In comparison to the RKUC model, the RHUC model predicts closer results to the results of Tamayol and Bahrami [26]. It should be noted that Tamayol and Bahrami [26] approximated the velocity field with a parabolic behavior at each section of the flow channel.

Although, as depicted in Figs. 7 and 8, the presented models RHUC and RKUC show fair agreement with Wang [20] and Tamayol and Bahrami [26], it could be useful to compare these models in the linear scale as opposed to the logarithmic scale. This is especially important because recognizing the differences between the results in the logarithmic scale may not be easy. However, the logarithmic scale has the benefit of covering a wide range of scales which exist in the permeability resutls. We investigated the variations of the ratios of the permeability results RHUC and RKUC, presented in Figs. 7 and 8, and the permeability results of Wang [20] and Tamayol and Bahrami [26] in those figures. Our investigation revealed that the deviation of the RHUC and RKUC results from those of Wang [20] and Tamayol and Bahrami [26] in Figs. 7 and 8 does not involve a change in the order of magnitude. Regarding the high sensitivity of the permeability values to volume fraction and aspect ratio (see Figs. 7 and 8), we consider this deviation in an acceptable range. To establish this argument, as an example, Fig. 9 shows the variation of the ratio $\kappa_x/(\kappa_x$ of Wang [20]) of the perpendicular permeability results κ_x and the perpendicular permeability component κ_x of Wang [20] [depicted in Fig. 7(a)], with volume fraction f for the selected values of the aspect ratio ζ. The results are shown for both permeability models RHUC and RKUC.

We now compare numerical values of the perpendicular permeabilities κ_x and κ_y for unit cells of elliptical cross sections, as obtained from our model, with results from previous studies. To the best of our knowledge, only Quinn [37] and Quinn *et al.* [38] have addressed such a problem, and only for the case of unit cells with infinitesimal ellipticity. By applying the perturbation method to Kuwabara's model, Quinn *et al.* [38] derived the permeability tensor for unit cells with infinitesimal ellipticity on their cross sections. As an example, upon considering the deviatoric strain tensor $\boldsymbol{D} = \varepsilon(\boldsymbol{e}_x \otimes \boldsymbol{e}_x - \boldsymbol{e}_y \otimes \boldsymbol{e}_y)$ (where $\boldsymbol{e}_x$ and $\boldsymbol{e}_y$ are the unit vectors in directions x and y, respectively), Quinn *et al.* [38] studied the change of the unit cell permeability due to the change of the unit cell cross section from a circular to an elliptical shape, controlled by the infinitesimal strain parameter ε, which also serves as the perturbation parameter. As studied by Quinn [37] and Quinn *et al.* [38], a distortion of the cross section of the unit cell from a circular to an elliptical shape emerges during the deformation of the proteoglycan network of articular cartilage, modelled as a system of cylindrical GAG molecules suspended in a solution. Such a consideration, of course, holds for any other system with similar microstructure. Notice that, in the small strain regime, the tensor $\boldsymbol{D}$ does not change the cross-sectional area of the unit cell. In fact, when a unit cell with initially circular cross section is compressed in the y direction, it is also stretched by the same amount in the x direction [38]. As the major and minor axes of the elliptical cross section of the unit cell in the perturbed Kuwabara model [38] are stretched and contracted by the strain ε respectively in the x and y directions (when $\varepsilon > 0$), the aspect ratio ζ_{ellip} in the elliptical unit cell models is given as $\zeta_{\text{ellip}} = (1-\varepsilon)/(1+\varepsilon)$, which is used as the aspect ratio of the elliptical unit cell models

in the present study (i.e., the EHUC and EKUC models) for comparing our results with those of Quinn *et al.* [38].

Furthemore, Quinn *et al.* [38] used the finite element method (FEM) to obtain the overall permeabilities of rectangular arrays, which constitutes another opportunity to compare our results for rectangular arrays. Quinn *et al.* [38] provided numerical comparisons between FEM results of rectangular arrays and the analytical results for unit cells with an elliptical cross section. For such a comparison, Quinn *et al.* [38] explained that the strain parameter ε must be related to the aspect ratio ζ_{rect} of the rectangular array via $\varepsilon = (\zeta_{\text{rect}}^{-1} - 1)/2$, which alternatively implies that $\zeta_{\text{rect}} = (1 + 2\varepsilon)^{-1}$. This is used as the aspect ratio of the rectangular unit cell models in the present study (i.e., the RHUC and RKUC models) for comparing our results with those of Quinn *et al.* [38].

Figure 10 shows the comparisons between the predicted results for the non-dimensional permeability κ_x/A_{uc} based on the RHUC and RKUC models for rectangular unit cells and the EHUC and EKUC models for elliptical unit cells with those of the perturbed Kuwabara model [38] for elliptical unit cells (linear theory with respect to ε) and the FEM [38] for rectangular arrays, given by Quinn *et al.* [38]. With A_{uc} being the unit cell cross-sectional area, and the property $f = \pi a^2/A_{\text{uc}}$, we have $\kappa_x/A_{\text{uc}} = \frac{4}{\pi} f\kappa_x/(4a^2)$. Similarly to Quinn *et al.* [38], three volume fractions, $f = 0.2$, $f = 0.3$, and $f = 0.4$, are considered.

Compared to other models, the EKUC model shows the closest match to the FEM data [38], particularly for smaller values of the volume fraction f. Thus, the presented EKUC model improves the model of Quinn *et al.* [38] for finite values of ε, or, in general, when the cross section of the unit cell possesses a finite ellipticity. The good consistency of Kuwabara's model [2] with the FEM results, compared to Happel's model [1], was observed by Quinn *et al.* [38] for square arrays. Among the examined models in Fig. 10 (i.e., the RHUC, RKUC, EHUC, and EKUC models) the RKUC (EHUC) model considerably underestimates (overestimates) the permeability values. Also, the EKUC and RHUC models show relatively close agreement for smaller values of the volume fraction f, but they deviate for larger values of f. It should be noted that the slopes of the EHUC model and the perturbed Kuwabara model [38] at $\varepsilon = 0$ do not match. In fact, the slope of the EHUC model shows better agreement with the slope of the FEM data [38] compared to the slope of the perturbed Kuwabara model [38].

VI. SUMMARY

The overall hydraulic permeability of a creeping fluid flow passing through a system of parallel impermeable cylindrical elements with orthotropic symmetry was studied using approximate analytical techniques. Two cases of arrays of cylinders were considered. In the first case, the cylinders were arranged on a regular rectangular lattice. In the second case, the cylinders were assumed to be arranged irregularly, while the cross section of a representative unit cell (containing a representative cylindrical core surrounded by interstitial fluid) is elliptical. Such an array, possessing an orthotropic overall permeability, can, for example, be attained as a result of deformation of an initially random distribution of arrays of parallel cylinders [37,38]. To completely describe the ortho-tropic permeability tensor of the system, it suffices to specify fluid flow permeabilities in three orthogonal directions: the direction parallel to the axes of the cylinders, and two directions perpendicular to the axes of the cylinders and oriented with the principal directions of the permeability tensor.

The previous studies [6,7,26] show weak sensitivity of parallel permeability to the lateral arrangement of parallel fibers (or the aspect ratio in rectangular arrays) and they [6,7] suggest that Happel's [1] parallel permeability relation can be a fair approximation even for nonrandom distribution of parallel fibers. In other words, when the solid volume fraction f is fixed, the orthotropy of an array, which is controlled by the aspect ratio ζ of the cross section of the unit cell, does not play an important role on the value of overall parallel permeability, especially for low values for the solid volume fraction f. This is also consistent with the observations previously made by Quinn [37] and Quinn *et al.* [38], indicating that the deviatoric

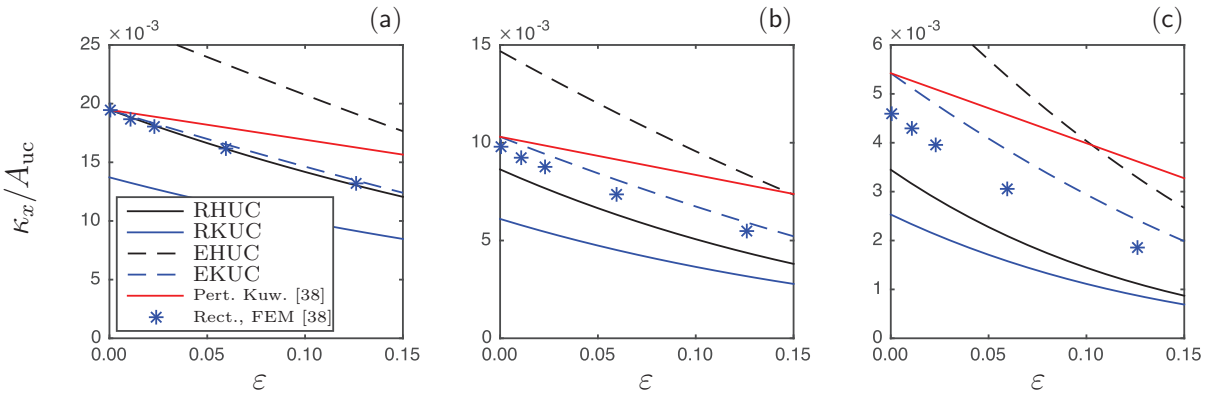

FIG. 10. Variation of the nondimensional perpendicular permeability component $\kappa_x/A_{\text{uc}} = \frac{4}{\pi} f\kappa_x/(4a^2)$ (normalized by the cross-sectional area A_{uc} of the unit cell) versus the deviatoric strain ε (defined as $\boldsymbol{D} = \varepsilon(\boldsymbol{e}_x \otimes \boldsymbol{e}_x - \boldsymbol{e}_y \otimes \boldsymbol{e}_y)$, where $\boldsymbol{D}$ is the deviatoric strain tensor in the small strain theory, and $\boldsymbol{e}_x$ and $\boldsymbol{e}_y$ are the unit vectors in the x and y directions). The RHUC, RKUC, EHUC, and EKUC models are considered for selected values of the volume fraction: (a) $f = 0.2$, (b) $f = 0.3$, and (c) $f = 0.4$. Comparisons with the perturbed Kuwabara's model and the FEM results for rectangular array in Quinn *et al.* [38] are provided.

strain responsible for distortion of the unit cell cross section of elliptical shape (while not altering its area) has no first-order contribution to the parallel permeability of arrays of parallel cylinders.

For perpendicular permeabilities, a key step was to replace an actual noncircular unit cell with an equivalent cylindrical unit cell for each perpendicular flow direction. However, in contrast with choosing an equivalent circular unit cell with the cross-sectional area equal to that of the original unit cell (as done by Happel [1]), it was proposed that, for each of the two perpendicular flows, the outer diameter of the equivalent unit cell be equal to the maximum width available for the fluid flow passing through the original, noncircular, unit cell with either rectangular or elliptical cross section. For the equivalent unit cells, the drag forces on the core cylinders are calculated using Happel's [1] and Kuwabara's [2] unit cell models, originally developed for random arrays of cylinders for which the unit cells are cylindrical. Next, having the drag forces for the two perpendicular flows, the overall permeabilities in the perpendicular directions are calculated by following the conventional method [1,37]. However, realizing that the drag force on each cylinder must be associated with the actual geometry of the unit cell, the original cross-sectional area of the unit cell (for both unit cells of rectangular and elliptical cross sections) is used for calculating the overall perpendicular permeabilities. This finally yields closed-form approximate analytical relations for perpendicular permeabilities of orthotropic arrays of parallel cylinders for which the unit cells have either rectangular or elliptical cross sections.

The accuracy of the developed relations for the perpendicular permeabilities of rectangular and irregular (with elliptical unit cell cross section) arrays is tested by comparing numerical values from our model against those from models available in the literature, either analytical (for rectangular unit cells [20,26] or for elliptical unit cells [38]) or FEM (for rectangular unit cells [38]). The results reveal that the proposed method has provided efficient and reliable closed-form permeability relations. Numerical comparisons indicate that the accuracy of the proposed relations increases for smaller solid volume fractions f and for aspect ratios closer to unity.

Regarding the observed efficiency of the present method, we believe that this technique can also be generalized to obtain simple solutions for more complex systems of nonrandom parallel cylinders, e.g., in which the cylindrical elements are permeable or inhomogeneous. In a forthcoming paper, we are going to exploit the model developed here to describe the permeability of the proteoglycan matrix of articular cartilage.

ACKNOWLEDGMENTS

This work was supported in part by Alberta Innovates-Technology Futures (Canada), through the AITF New Faculty Program (S.F.), Alberta Innovates-Health Solutions (Canada), through the AIHS Postgraduate Fellowship Program (M.M.) and the AIHS Sustainability Program (S.F.), the Natural Sciences and Engineering Research Council of Canada, through the NSERC Discovery Program (R.J.M., W.H., S.F.) and the NSERC CREATE Training Program for Biomedical Engineers for the 21st Century (M.M.), The Canadian Institutes of Health Research (CIHR) (W.H.), The Canada Research Chair Program (CRC Tier I for Cellular and Molecular Biomechanics) (W.H.), and the Killam Foundation (Killam Memorial Chair) (W.H.).

[1] J. Happel, AlChE J. **5**, 174 (1959).
[2] S. Kuwabara, J. Phys. Soc. Jpn. **14**, 527 (1959).
[3] H. Hasimoto, J. Fluid Mech. **5**, 317 (1959).
[4] A. Sangani and A. Acrivos, Int. J. Multiph. Flow **8**, 193 (1982).
[5] F. S. Henry and T. Ariman, Part. Sci. Technol. **1**, 1 (1983).
[6] J. Drummond and M. Tahir, Int. J. Multiph. Flow **10**, 515 (1984).
[7] G. W. Jackson and D. F. James, Can. J. Chem. Eng. **64**, 364 (1986).
[8] A. S. Sangani and C. Yao, Phys. Fluids **31**, 2435 (1988).
[9] N. J. Meegoda, I. P. King, and K. Arulanandan, Int. J. Numer. Anal. Meth. Geomech. **13**, 575 (1989).
[10] D. Edwards, M. Shapiro, P. Bar-Yoseph, and M. Shapira, Phys. Fluids A **2**, 45 (1990).
[11] B. Gebart, J. Compos. Mater. **26**, 1100 (1992).
[12] B. T. Åström, R. B. Pipes, and S. G. Advani, J. Compos. Mater. **26**, 1351 (1992).
[13] M. Bruschke and S. Advani, J. Rheol. **37**, 479 (1993).
[14] C. K. Ghaddar, Phys. Fluids **7**, 2563 (1995).
[15] F. R. Phelan and G. Wise, Compos. Part A **27**, 25 (1996).
[16] S. Ranganathan, F. R. Phelan, and S. G. Advani, Polym. Compos. **17**, 222 (1996).
[17] Y. Zhu, P. J. Fox, and J. P. Morris, Int. J. Numer. Anal. Meth. Geomech. **23**, 881 (1999).
[18] C. Wang, Appl. Math. Modell. **23**, 219 (1999).
[19] F. Alcocer, V. Kumar, and P. Singh, Phys. Rev. E **59**, 711 (1999).
[20] C. Wang, Fluid Dyn. Res. **29**, 65 (2001).
[21] C. Wang, Fluid Dyn. Res. **32**, 233 (2003).
[22] M. Hellou, J. Martinez, and M. El Yazidi, Mech. Res. Commun. **31**, 97 (2004).
[23] V. Kirsh, Colloid J. **68**, 261 (2006).
[24] M. P. Sobera and C. R. Kleijn, Phys. Rev. E **74**, 036301 (2006).
[25] A. Nabovati, E. W. Llewellin, and A. C. Sousa, Compos. Part A **40**, 860 (2009).
[26] A. Tamayol and M. Bahrami, Int. J. Heat Mass Transfer **52**, 2407 (2009).
[27] J. G. I. Hellstrom, P. J. P. Jonsson, and T. S. Lundstrom, J. Porous Media **13**, 1073 (2010).
[28] A. Tamayol and M. Bahrami, Phys. Rev. E **83**, 046314 (2011).
[29] K. Yazdchi, S. Srivastava, and S. Luding, Int. J. Multiph. Flow **37**, 956 (2011).
[30] R. Yip, D. F. James, and I. G. Currie, Exp. Fluids **51**, 801 (2011).
[31] A. C. Baytas, D. Erdem, H. Acar, O. Cetiner, and H. Basci, J. Porous Media **15**, 1009 (2012).
[32] A. Tamayol, J. Yeom, M. Akbari, and M. Bahrami, Int. J. Heat Mass Transfer **58**, 420 (2013).

[33] D. Shou, L. Ye, and J. Fan, J. Compos. Mater. **49**, 1753 (2015).
[34] Y. Li and C.-W. Park, Chem. Eng. Sci. **54**, 633 (1999).
[35] Y. Li and C.-W. Park, Adv. Colloid Interface Sci. **87**, 1 (2000).
[36] C. DeValve and R. Pitchumani, Compos. Sci. Technol. **72**, 1500 (2012).
[37] T. M. Quinn, Ph.D. thesis, Massachusetts Institute of Technology, 1996.
[38] T. Quinn, P. Dierickx, and A. Grodzinsky, J. Biomech. **34**, 1483 (2001).
[39] A. Maroudas, Biophys. J. **8**, 575 (1968).
[40] H. T. Nia, I. S. Bozchalooi, Y. Li, L. Han, H.-H. Hung, E. Frank, K. Youcef-Toumi, C. Ortiz, and A. Grodzinsky, Biophys. J. **104**, 1529 (2013).
[41] P. J. Flory, Trans. Faraday Soc. **57**, 829 (1961).